ELSEVIER

Isolation and single-crystal X-ray structure analysis of the catalyst–substrate host–guest complexes $[C_6H_6 \subset H_3Ru_3\{C_6H_5(CH_2)_nOH\}(C_6Me_6)_2(O)]^+$ $(n = 2, 3)$
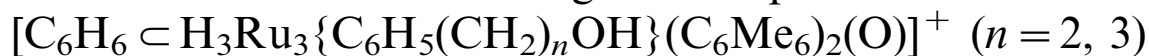
Ludovic Vieille-Petit, Bruno Therrien, Georg Süss-Fink *, Thomas R. Ward

Institut de Chimie, Université de Neuchâtel, Case Postale 2, CH-2007 Neuchâtel, Switzerland

Dedicated to Professor Ernst Otto Fischer on the occasion of his 85th birthday

Abstract

The trinuclear arene-ruthenium cluster cations $[H_3Ru_3\{C_6H_5(CH_2)_nOH\}(C_6Me_6)_2(O)]^+$ (**3**: $n = 2$, **4**: $n = 3$) have been synthesised from the dinuclear precursor $[H_3Ru_2(C_6Me_6)_2]^+$ and the mononuclear complexes $[\{C_6H_5(CH_2)_nOH\}Ru(H_2O)_3]^{2+}$ in aqueous solution, isolated and characterised as the hexafluorophosphate or tetrafluoroborate salts. Both **3** and **4** are derivatives of the parent cluster cation $[H_3Ru_3(C_6H_6)(C_6Me_6)_2(O)]^+$ (**1**) which was found to catalyse the hydrogenation of benzene to give cyclohexane under biphasic conditions. The mechanism postulated for this catalytic reaction ('supramolecular cluster catalysis'), involving the hydrophobic pocket spanned by the three arene ligands in **1**, was based on the assumption that the substrate molecule benzene is hosted inside the hydrophobic pocket of the cluster molecule to form a catalyst–substrate host–guest complex in which the hydrogenation of the substrate takes place. With the analogous cluster cations **3** and **4**, containing a $(CH_2)_nOH$ side-arm ($n = 2, 3$) as substituent at the benzene ligand, it was possible to isolate the cationic host–guest complexes as the hexafluorophosphate or tetrafluoroborate salts. The single-crystal X-ray structure analyses of $[C_6H_6 \subset \mathbf{3}][PF_6]$ and $[C_6H_6 \subset \mathbf{4}][BF_4]$, compared to that of $[\mathbf{3}][PF_6]$ show that the substrate molecule benzene is indeed held inside the hydrophobic pocket of **3** and **4**, the angle between the metal (Ru$_3$) plane and the aromatic plane being 67° and 89°, respectively.
© 2003 Elsevier Science B.V. All rights reserved.

Keywords: Cluster catalysis; Supramolecular effects; Intermolecular interactions; Second sphere coordination; Arene hydrogenation; Biphasic catalysis; Hydrophobic forces; Molecular recognition; Host–guest complexes

1. Introduction

Organometallic catalysis most often proceeds through a catalytic cycle, which involves the *coordination of the substrate*, either by ligand substitution or by oxidative addition, *transformation of the coordinated substrate*, and *liberation of the product*, either by decoordination or by reductive elimination [1]. Classical examples which have been studied in great detail are the hydrogenation of olefins with Wilkinson's catalyst [2] and the carbonylation of methanol with rhodium iodide (Monsanto Process) [3]. The complete characterisation of the intermediates of the latter process and the proposal of a well-established catalytic cycle represents one of the triumphs of organometallic chemistry [4]. In all these reactions, the elementary steps of the catalytic process are believed to occur within the *first* coordination sphere of the organometallic catalyst [5].

Only recently a catalytic mechanism without coordination of the substrate to the metal centre of the catalyst molecule has been considered [6,7], based on accumulating evidence for hydrogen transfer within merely hydrogen-bonded substrate–catalyst complexes in the case of catalytic ketone transfer hydrogenation reactions [8] and for oxygen transfer via direct olefin attack to the oxo ligand of the catalyst in epoxidation reactions [9].

We discovered last year that the water-soluble cluster cations $[H_3Ru_3(C_6H_6)(C_6Me_6)_2(O)]^+$ (**1**) and

$[H_2Ru_3(C_6H_6)(C_6Me_6)_2(O)(OH)]^+$ (**2**) are highly active in the catalytic hydrogenation of benzene to cyclohexane under biphasic conditions [10,11]. Mass spectroscopic studies and modelling studies suggest that the substrate molecule is incorporated in the hydrophobic pocket spanned by the three arene ligands in **1** and in **2**, suggesting the catalytic reaction to occur within this host–guest complex without prior coordination of the substrate ('supramolecular cluster catalysis') [12,13].

$$C_6H_6 + 3H_2 \rightarrow C_6H_{12}$$

All experimental findings are in accordance with the concept of supramolecular cluster catalysis based on molecular modelling. The only missing link was the direct observation of the catalyst–substrate host–guest complexes $[C_6H_6 \subset 1]^+$ and $[C_6H_6 \subset 2]^+$ for which we had so far only mass spectroscopic evidence. However, by introducing a $(CH_2)_nOH$ side-arm as a substituent at the benzene ligand to give the cluster cations $[H_3Ru_3\{C_6H_5(CH_2)_nOH\}(C_6Me_6)_2(O)]^+$ (**3**: $n = 2$, **4**: $n = 3$), we were now able to crystallise the host–guest complexes with a substrate molecule inside the hydrophobic pocket. In this paper we report on the isolation and single-crystal X-ray structure analyses of the catalyst–substrate host–guest complexes $[C_6H_6 \subset 3][PF_6]$ and $[C_6H_6 \subset 4][BF_4]$.

2. Results and discussion

The trinuclear cations $[H_3Ru_3\{C_6H_5(CH_2)_nOH\}(C_6Me_6)_2(O)]^+$ (**3**: $n = 2$, **4**: $n = 3$), derivatives of **1**, have been synthesised in aqueous solution from the dinuclear precursor $[H_3Ru_2(C_6Me_6)_2]^+$ [14,15] and $[\{C_6H_5(CH_2)_nOH\}Ru(H_2O)_3]^{2+}$, mononuclear analogues of the known cation $[(C_6H_6)Ru(H_2O)_3]^{2+}$ [16] (Scheme 1).

Both, **3** and **4** are catalytically active for the hydrogenation of benzene under biphasic conditions; although they are less active than **1** (TOF 140 h^{-1} for **3**, 125 h^{-1}
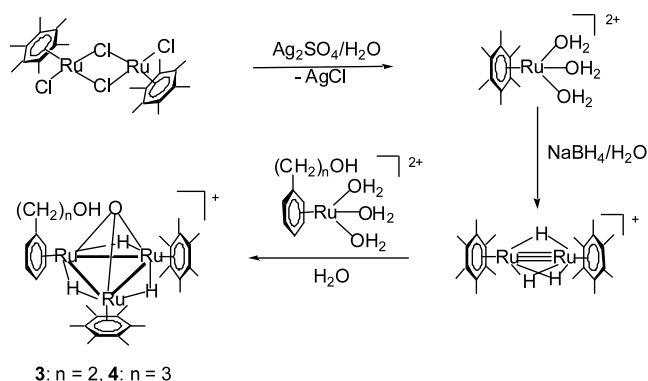
for **4**, as compared to 190 h^{-1} for **1**) under the same conditions (catalyst/substrate ratio 1:1000, 110 °C, 60 bar H$_2$, 4 h), they show the same catalytic features as **1**.

From acetone solutions containing **3** or **4** in the presence of benzene, the expected catalyst–substrate host–guest complexes have been isolated as the hexafluorophosphate or the tetrafluoroborate salts $[C_6H_6 \subset 3][PF_6]$ and $[C_6H_6 \subset 4][BF_4]$. For comparison, the empty cluster cation **3** was also isolated as the hexafluorophosphate salt $[3][PF_6]$. A comparative X-ray study of $[C_6H_6 \subset 3][PF_6]$, $[C_6H_6 \subset 4][BF_4]$ and $[3][PF_6]$ allows the analysis of the host–guest intermediates postulated for supramolecular cluster catalysis [12,13].

The molecular structures of $[3]^+$ and $[C_6H_6 \subset 3]^+$ are shown in Fig. 1; the molecular structure of $[C_6H_6 \subset 4]^+$ is presented in Fig. 2. In all cases, the metal core consists of three ruthenium atoms, the three Ru–Ru distances being in accordance with a metal–metal single bond. The three ruthenium atoms are capped by a μ$_3$-oxo ligand which is almost symmetrically coordinated. The three hydrido ligands bridging the three ruthenium–ruthenium bonds could be localised and fully refined. Selected bond lengths and angles are listed in Table 1. In all cases the triruthenium framework is comparable, showing similar geometric parameters, differences appear only in the periphery (Scheme 2).

Clusters **3** and **4** differ by the existence of intra- or intermolecular hydrogen bonds in the solid state: The presence of a CH$_2$CH$_2$OH side-arm allows **3** to form a strong intramolecular hydrogen bond with the μ$_3$-oxo ligand, the O···O distances are 2.672(4) for $[3]^+$ and 2.698(2) Å for $[C_6H_6 \subset 3]^+$ with O–H···O angles of 171.9° and 161.5°, respectively. Interestingly, no such intramolecular hydrogen bond with the CH$_2$CH$_2$CH$_2$OH side-arm is observed in $[C_6H_6 \subset 4]^+$. Instead, in the solid state, cluster **4** exists as centrosymmetric μ$_3$-O···H$_2$O···HO–CH$_2$– hydrogen-bonded dimers, a water molecule being hydrogen-bonded to the μ$_3$-O ligand [O···O distance 2.760(3) Å, O–H···O angle 169.7°] and to the (CH$_2$)$_3$OH side-arm [O···O distance 2.785(3) Å, O–H···O angle 167.2°] (Fig. 3).

In the host–guest complexes $[C_6H_6 \subset 3]^+$ and $[C_6H_6 \subset 4]^+$, a benzene molecule is observed inside the hydrophobic pocket. It is well known that π systems have a great influence on the three-dimensional molecular and crystal structures; thus benzene molecules can interact with neighbouring arene moieties by π stacking [17]. In the molecular structures of $[C_6H_6 \subset 3]^+$ and $[C_6H_6 \subset 4]^+$ we find, however, no π stacking: The guest molecule interacts in both cases weakly with the host only by hydrophobic and van der Waals contacts. However, in the crystal structure of $[C_6H_6 \subset 4][BF_4]\cdot$ H$_2$O$\cdot$0.5 C$_6$H$_6$, a second benzene molecule is present outside of the hydrophobic pocket, which is in π stacking interaction with the guest benzene molecule ('T-shaped mode') as well as with one of the two
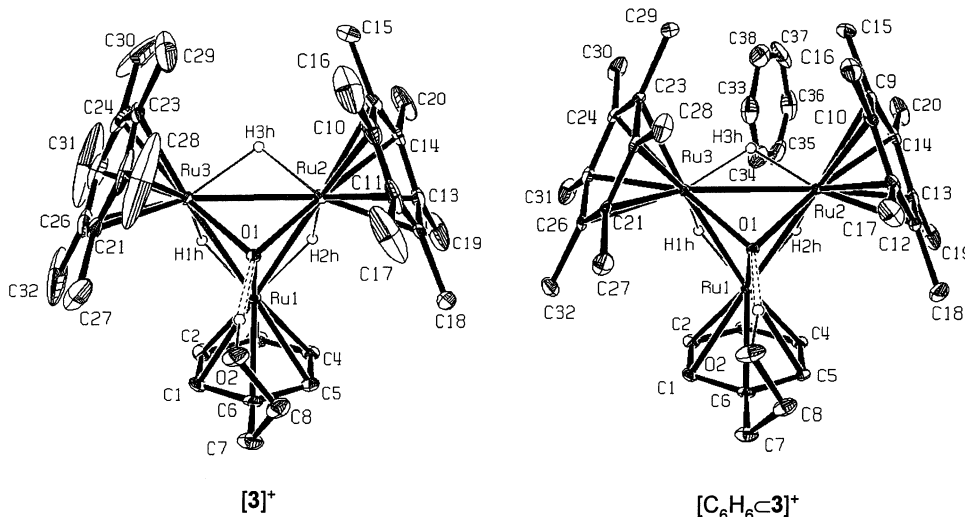
Scheme 1. Synthesis of the trinuclear cluster cations **3** and **4** from the dinuclear precursor $[H_3Ru_2(C_6Me_6)_2]^+$ and the mononuclear complexes $[\{C_6H_5(CH_2)_nOH\}Ru(H_2O)_3]^{2+}$ ($n = 2, 3$) in aqueous solution.

Fig. 1. Molecular structure of cations **3** at 25% probability level, H atoms and PF_6 omitted for clarity.
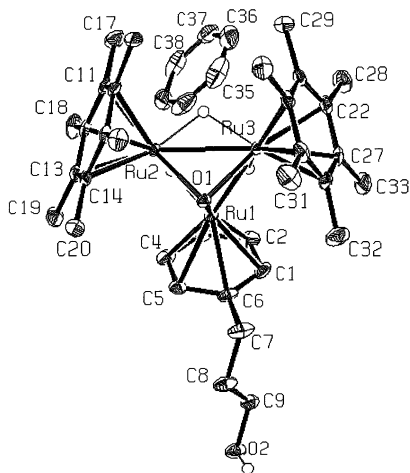
Fig. 2. Molecular structure of $[C_6H_6 \subset 4]^+$ at 25% probability level, H atoms, H_2O and BF_4 omitted for clarity.

Table 1
Selected bond lengths (Å) and angles (°) for $[3]^+$, $[C_6H_6 \subset 3]^+$, and $[C_6H_6 \subset 4]^+$

	$[3]^+$	$[C_6H_6 \subset 3]^+$	$[C_6H_6 \subset 4]^+$
Bond lengths			
Ru(1)–Ru(2)	2.7463(5)	2.7508(3)	2.7488(5)
Ru(2)–Ru(3)	2.8090(5)	2.7938(4)	2.7904(5)
Ru(1)–Ru(3)	2.7535(5)	2.7528(3)	2.7534(5)
Ru(1)–O(1)	2.007(3)	2.007(2)	2.012(2)
Ru(2)–O(1)	2.002(2)	2.004(2)	2.012(2)
Ru(3)–O(1)	2.002(3)	2.007(2)	2.011(2)
Bond angles			
Ru(1)–Ru(2)–Ru(3)	59.41(1)	59.530(7)	59.608(14)
Ru(1)–Ru(3)–Ru(2)	59.16(1)	59.458(7)	59.446(13)
Ru(2)–Ru(1)–Ru(3)	61.43(1)	61.012(8)	60.946(12)
Ru(1)–O(1)–Ru(2)	86.47(10)	86.58(6)	86.18(7)
Ru(1)–O(1)–Ru(3)	86.77(11)	86.59(6)	86.38(8)
Ru(2)–O(1)–Ru(3)	89.11(10)	88.29(6)	87.82(7)

hexamethylbenzene ligands ('slipped parallel mode'); the distances observed between the centres of the interacting π systems (5.26 and 3.77 Å) are in good agreement with the theoretical values calculated for these π stacking modes [17] (Fig. 4).

In our previous modelling study [12], where the benzene substrate was docked in the hydrophobic pocket of **1** and **2** in a parallel fashion with respect to the metal plane, we found streric repulsions between the hydrogen atoms of the benzene substrate and those of the arene ligands in the case of **1**, suggesting an inclined orientation of the benzene molecule in the hydrophobic pocket of **1**. The crystallographic results do indeed confirm this hypothesis: In $[C_6H_6 \subset 3]^+$, the angle formed by the C_6 plane and the Ru_3 plane is 66.78(7)°, while it is 88.63(9)° in $[C_6H_6 \subset 4]^+$, the guest molecule being held almost upright in the hydrophobic pocket (Fig. 5).

The shortest distances between the metal-bound hydrogen atoms and the closest carbon atoms of the benzene guest molecule are 3.49 and 3.69 Å in $[C_6H_6 \subset 3]^+$, and 3.26 and 3.77 Å in $[C_6H_6 \subset 4]^+$ (Fig. 6). These
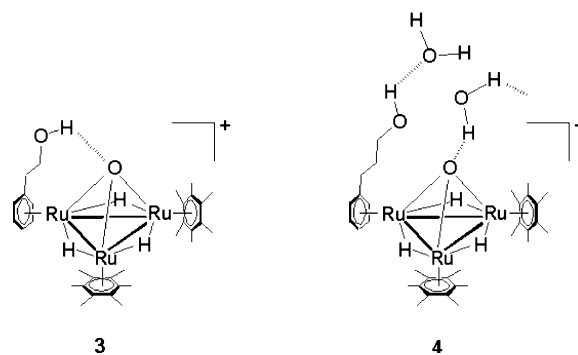
Scheme 2. Hydrogen bonding in the trinuclear cluster cations $[H_3Ru_3\{C_6H_5(CH_2)_2OH\}(C_6Me_6)_2(O)]^+$ (**3**) (intramolecular) and $[H_3Ru_3\{C_6H_5(CH_2)_3OH\}(C_6Me_6)_2(O)]^+$ (**4**) (intermolecular).
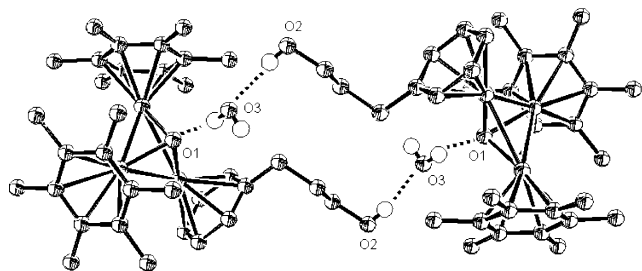
Fig. 3. Hydrogen-bonded dimers of [C$_6$H$_6$ $\subset$ **4**][BF$_4$]·H$_2$O·0.5C$_6$H$_6$.
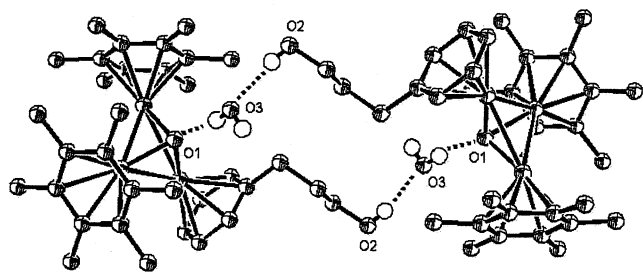

Fig. 4. Capped sticks representation of the π interaction in **4**, (A) guest benzene molecules; (B) solvate benzene molecule and (C) hexamethylbenzene ligand.

close contacts between the guest and the host inside the hydrophobic pocket may favour the hydrogen transfer from the catalyst to the substrate in the catalytic process.

3. Experimental

3.1. General

All manipulations were carried out by routine under nitrogen atmosphere. De-ionised water and organic solvents were degassed and saturated with nitrogen

prior to use. NMR spectra were recorded on a Varian 200 MHz spectrometer. IR spectra were recorded on a Perkin–Elmer FT-IR spectrometer (4000–400 cm^{-1}). Microanalyses were carried out by the Laboratory of Pharmaceutical Chemistry, University of Geneva (Switzerland). Electro-spray mass spectra were obtained in positive-ion mode with an LCQ Finnigan mass spectrometer. Organic products were analysed by gas chromatography (GC) on a DANI 86.10 HT GC using a CHROMPACK Carbowax WCOT fused silica column. The starting dinuclear dichloro complexes [Ru(C$_6$-Me$_6$)Cl$_2$]$_2$ [18] and [Ru{C$_6$H$_5$(CH$_2$)$_3$OH}Cl$_2$]$_2$ [19] were prepared according to published methods. C$_6$H$_7$(CH$_2$)$_2$OH was prepared by standard *Birch* reduction [20] of commercially available C$_6$H$_5$(CH$_2$)$_2$OH (Aldrich).

3.2. Syntheses

3.2.1. [Ru{C$_6$H$_5$(CH$_2$)$_2$OH}Cl$_2$]$_2$

To a solution of ruthenium trichloride hydrate (840 mg, 3.2 mmol) in ethanol (70 ml) was added C$_6$H$_7$(CH$_2$)$_2$OH (2 g, 16.1 mmol), and the mixture was refluxed overnight. The orange precipitate was filtered, washed with ether, and dried under vacuum to give [Ru{C$_6$H$_5$(CH$_2$)$_2$OH}Cl$_2$]$_2$. Yield: 1.35 g (72%).

Spectroscopic data: δ ^{1}H (200 MHz, dmso-d_6) 6.03–5.74 (m, 5H, C$_6$H$_5$), 4.78 (br s, 1H, O*H*), 3.71 (t, 2H, C*H$_2$*OH), 2.57 (t, 2H, C*H$_2$*CH$_2$OH). δ ^{13}C{^{1}H} (50 MHz, dmso-d_6) 105.8 (Ru–*C$_6$*H$_5$), 89.1 (Ru–*C$_6$*H$_5$), 86.7 (Ru–*C$_6$*H$_5$), 84.3 (Ru–*C$_6$*H$_5$), 60.5 (*C*H$_2$OH), 36.8 (*C*H$_2$CH$_2$OH). MS (ESI positive mode, dmso): *m/z*: 557 [M$^+$ −CH$_2$OH]. Anal. Found: C, 32.27; H, 3.41. Calc. for C$_{16}$H$_{20}$O$_2$Cl$_4$Ru$_2$: C, 32.67; H, 3.43%.
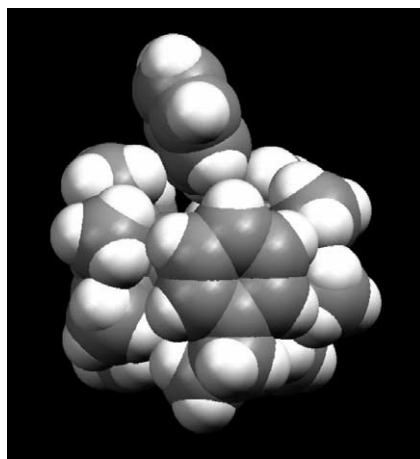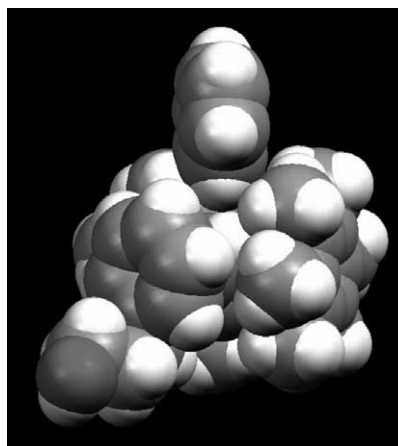
$[C_6H_6 \subset \mathbf{3}]^+$ $[C_6H_6 \subset \mathbf{4}]^+$

Fig. 5. Space filling representation of the host–guest complexes [C$_6$H$_6$ $\subset$ **3**]$^+$ and [C$_6$H$_6$ $\subset$ **4**]$^+$, based on the X-ray data, showing the benzene host (at the top) penetrating the hydrophobic pocket of **3** and **4**.
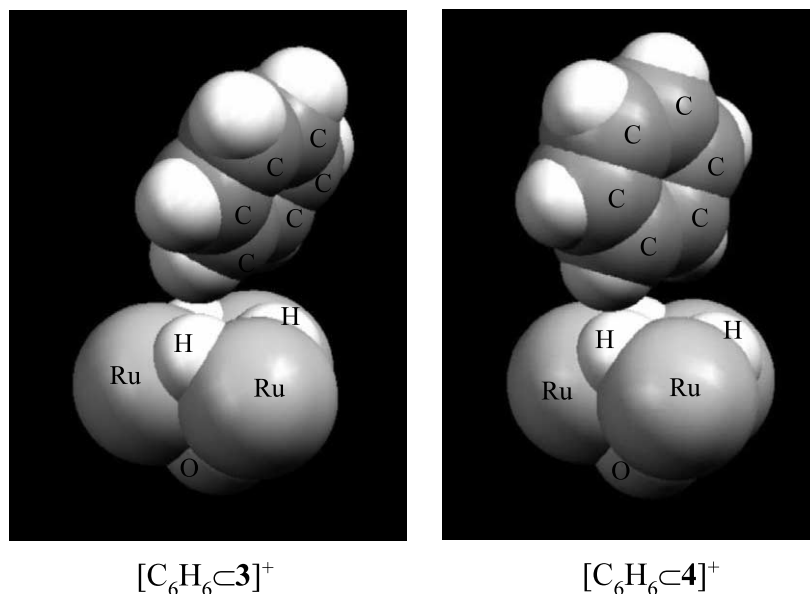
$[C_6H_6 \subset \mathbf{3}]^+$

$[C_6H_6 \subset \mathbf{4}]^+$

Fig. 6. Space filling representation of the host–guest complexes $[C_6H_6 \subset \mathbf{3}]^+$ and $[C_6H_6 \subset \mathbf{4}]^+$ with the benzene guest (top) approaching the Ru_3 plane, the arene ligands being omitted for clarity.

3.2.2. $[H_3Ru_3\{C_6H_5(CH_2)_nOH\}(C_6Me_6)(O)]^+$ ($\mathbf{3}$: $n = 2$, $\mathbf{4}$: $n = 3$)

A mixture of $[Ru(C_6Me_6)Cl_2]_2$ (200 mg, 0.3 mmol) and Ag_2SO_4 (188 mg, 0.6 mmol) in water (20 ml) was stirred in the dark for 1 h. During this period the mixture was treated several times with ultrasound, until the orange solid was completely dissolved. The white precipitate (AgCl) was removed by filtration from the yellow solution containing $[Ru(C_6Me_6)(H_2O)_3]^{2+}$. An aqueous solution containing $NaBH_4$ (50 mg, 1.3 mmol, 10 ml H_2O) was added dropwise to this yellow solution. The solution turned dark-red due to the formation of $[Ru_2(C_6Me_6)_2(\mu_2\text{-}H)_3]^+$. After filtration, solid $[Ru\{C_6H_5(CH_2)_nOH\}Cl_2]_2$ (164 mg, 0.28 mmol for $n = 2$ and 168 mg, 0.28 mmol for $n = 3$) was added. The mixture was heated to 60 °C for 50 h in a closed pressure Schlenk tube. The resulting red solution was filtered, and a large excess of $NaBF_4$ or KPF_6 was added to precipitate the corresponding salts $[\mathbf{3}][BF_4]$ or $[\mathbf{3}][PF_6]$ and $[\mathbf{4}][BF_4]$ or $[\mathbf{4}][PF_6]$. The precipitate was centrifuged, dissolved in CH_2Cl_2, filtered on celite to eliminate the excess of $NaBF_4$ or KPF_6 and purified on silica-gel plates (eluent: CH_2Cl_2/acetone 2:1). Yield: 30–40% for $\mathbf{3}$ and 35–43% for $\mathbf{4}$.

Spectroscopic data for $\mathbf{3}$: δ ^1H (200 MHz, acetone-d_6) 6.62 (t, 1H, CH_2CH_2OH), 6.10–5.38 (m, 5H, C_6H_5), 3.95 (m, 2H, CH_2CH_2OH), 2.57 (t, 2H, CH_2CH_2OH), 2.34 (s, 36H, $C_6(CH_3)_6$), −19,29 (d, 2H, Ru hydride), −19.80 (t, 1H, Ru hydride). δ $^{13}C\{^1H\}$ (50 MHz, acetone-d_6) 108.8 (Ru–C_6H_5), 95.1 (Ru–$C_6(CH_3)_6$), 85.9 (Ru–C_6H_5), 79.0 (Ru–C_6H_5), 76.4 (Ru–C_6H_5), 60.3 (CH_2CH_2OH), 36.8 (CH_2CH_2OH), 17.3 ($C_6(CH_3)_6$). MS (ESI positive mode, acetone): m/z: 770 $[M^+ + 2H]$. IR (KBr): 3182 cm^{-1}, ν(O–H). Anal. Found: C, 44.23;

H, 5.65. Calc. for $C_{32}H_{49}$ $BF_4O_2Ru_3 \cdot H_2O$: C, 43.99; H, 5.88%.

Spectroscopic data for $\mathbf{4}$: δ ^1H (200 MHz, acetone-d_6) 5.94 to 5.43 (m, 5H, C_6H_5), 3.96 (t, 1H, $CH_2CH_2CH_2OH$), 3.68 (m, 2H, $CH_2CH_2CH_2OH$), 2.58 (m, 2H, $CH_2CH_2CH_2OH$), 2.32 (s, 36H, $C_6(CH_3)_6$), 2.00 (t, 2H, $CH_2CH_2CH_2OH$), −19.25 (d, 2H, Ru hydride), −19.92 (t, 1H, Ru hydride). δ $^{13}C\{^1H\}$ (50 MHz, acetone-d_6) 106.8 (Ru–C_6H_5), 94.9 (Ru–$C_6(CH_3)_6$), 85.4 (Ru–C_6H_5), 79.7 (Ru–C_6H_5), 77.8 (Ru–C_6H_5), 60.8 ($CH_2CH_2CH_2OH$), 32.9 ($CH_2CH_2CH_2OH$), 30.7 ($CH_2CH_2CH_2OH$), 17.4 ($C_6(CH_3)_6$). MS (ESI, positive mode, acetone): m/z: 783 $[M^+ + H]$. IR (KBr): 3426 cm^{-1}, ν(O–H). Anal. Found: C, 45.02; H, 6.05. Calc. for $C_{33}H_{51}$ $BF_4O_2Ru_3 \cdot$ H_2O: C, 44.65; H, 6.02%.

3.3. Catalytic runs

In a typical experiment, a solution of $[\mathbf{3}][BF_4]$ or $[\mathbf{4}][BF_4]$ (10 mg) in 10 ml of degassed water was placed in a 100 ml stainless steel autoclave, and the substrate benzene was added with a 1/1000 ratio catalyst/substrate. After purging four times with hydrogen, the autoclave was pressurised with hydrogen (60 bar) and heated to 110 °C in an oil bath under vigorous stirring. After 4 h, the autoclave was placed in an ice-bath and the pressure released. The two-phase system was separated by decanting. The aqueous phase containing the catalyst was evaporated to dryness under vacuum, and the residue was analysed by NMR and mass spectroscopy. The organic phase containing cyclohexane and benzene was analysed by NMR and GC.

Table 2
Crystallographic and selected experimental data of [**3**][PF$_6$], [C$_6$H$_6$ ⊂ **3**][PF$_6$], and [C$_6$H$_6$ ⊂ **4**][BF$_4$]

	[**3**][PF$_6$]	[C$_6$H$_6$ ⊂ **3**][PF$_6$]	[C$_6$H$_6$ ⊂ **4**][BF$_4$]·H$_2$O·0.5C$_6$H$_6$
Chemical formula	C$_{38}$H$_{55}$F$_6$O$_2$PRu$_3$	C$_{32}$H$_{49}$F$_6$O$_2$PRu$_3$	C$_{42}$H$_{62}$BF$_4$O$_3$Ru$_3$
Formula weight	992.00	913.89	1004.94
Temperature (K)	153(2)	153(2)	153(2)
Crystal system	monoclinic	triclinic	triclinic
Space group	$P2_1/n$	$P\bar{1}$	$P\bar{1}$
Crystal colour and shape	orange block	orange plate	orange block
Crystal size	$0.25 \times 0.20 \times 0.15$	$0.60 \times 0.50 \times 0.04$	$0.40 \times 0.30 \times 0.30$
a (Å)	10.8408(7)	10.6164(10)	12.0641(16)
b (Å)	10.6552(5)	11.1725(11)	13.2920(17)
c (Å)	32.734(2)	14.4353(15)	13.3493(17)
α (°)	90	100.650(12)	94.712(15)
β (°)	95.671(8)	99.462(12)	103.460(15)
γ (°)	90	91.061(12)	96.396(15)
V (Å^3)	3762.7(4)	1657.7(3)	2055.9(5)
Z	4	2	2
D_{calc} (g cm^{-3})	1.751	1.831	1.623
μ (mm^{-1})	1.294	1.460	1.143
Scan range (°)	$4.02 < 2\theta < 51.88$	$4.26 < 2\theta < 51.84$	$4.10 < 2\theta < 52.06$
Unique reflections	7110	5988	7467
Reflections used [$I > 2\sigma(I)$]	6452	4997	6489
R_{int}	0.0590	0.0321	0.0303
Final R indices [$I > 2\sigma(I)$]	$R_1 = 0.0241$, $wR_2 = 0.0643$	$R_1 = 0.0345$, $wR_2 = 0.0871$	$R_1 = 0.0236$, $wR_2 = 0.0608$
R indices (all data)	$R_1 = 0.0275$, $wR_2 = 0.0668$	$R_1 = 0.0424$, $wR_2 = 0.0894$	$R_1 = 0.0297$, $wR_2 = 0.0727$
Goodness-of-fit	1.056	1.012	1.125
Max, Min $\Delta\rho$ (e Å^{-3})	0.649, -0.700	1.006, -0.759	0.682, -0.836

3.4. X-ray crystallography

Crystals of [**3**][PF$_6$], [C$_6$H$_6$ ⊂ **3**][PF$_6$], and [C$_6$H$_6$ ⊂ **4**][BF$_4$] were mounted on a Stoe Image Plate Diffraction system equipped with a ϕ circle goniometer, using Mo–K$_\alpha$ graphite monochromated radiation ($\lambda = 0.71073$ Å) with ϕ range 0–200°, increment between 0.7° and 1.7°, $D_{max} - D_{min} = 12.45$–0.81 Å. The structures were solved by direct methods using the program SHELXS-97 [21]. The refinement and all further calculations were carried out using SHELXL-97 [22]. In [C$_6$H$_6$ ⊂ **4**][BF$_4$] the hydrogen atoms attached to the water molecule and to the oxygen of the alcohol function, as well as the hydrides have been found as electron density peaks and refined while the remaining hydrogen atoms were included in calculated positions and treated as riding atoms using the SHELXL default parameters. The same treatment has been applied to [**3**][PF$_6$] and [C$_6$H$_6$ ⊂ **3**][PF$_6$], the hydrogen of the alcohol function and the hydrides have been found from Fourier difference maps and constrained to their positions, while the remaining hydrogen atoms were included in calculated positions and treated as riding atoms using the SHELXL default parameters. All non-H atoms were refined anisotropically, using weighted full-matrix least-square on F^2. Crystallographic details are summarised in Table 2. Figures were drawn with ORTEP [23].

4. Supplementary material

Full tables of atomic parameters, bond lengths and angles are deposited at the Cambridge Crystallographic Data Centre, 12 Union Road, Cambridge CB2 1EZ, UK, Deposition numbers: [**3**][PF$_6$] 203563, [C$_6$H$_6$ ⊂ **3**][PF$_6$] 203562 and [C$_6$H$_6$ ⊂ **4**][BF$_4$] 203564.

References

[1] (a) S. Bhaduri, D. Mukesh, Homogeneous Catalysis, Wiley-Interscience, New York, 2000;
(b) B. Cornils, W.A. Herrmann, Applied Homogeneous Catalysis with Organometallic Compounds, VCH, Weinheim, 1996;
(c) G.W. Parshall, S.D. Ittel, Homogeneous Catalysis, Wiley-Interscience, New York, 1992.
[2] B.R. James, Adv. Organomet. Chem. 17 (1979) 319.
[3] D. Forster, Adv. Organomet. Chem. 17 (1979) 255.

[4] P.M. Maitlis, A. Haynes, G.J. Sunley, M.J. Howard, J. Chem. Soc. Dalton Trans. (1996) 2187.

[5] W.A. Herrmann, B. Cornils, Angew. Chem. Int. Ed. Engl. 36 (1997) 1048.

[6] (a) R. Noyori, T. Ohkuma, Angew. Chem. 113 (2001) 41;
(b) R. Noyori, T. Ohkuma, Angew. Chem. Int. Ed. 40 (2001) 40;
(c) D.A. Alonso, P. Brandt, S.J.M. Nordin, P.G. Andersen, J. Am. Chem. Soc. 121 (1999) 9580.

[7] E.N. Jacobsen, M.H. Wu, in: E.N. Jacobsen, A. Pfaltz, H. Yamamoto (Eds.), Comprehensive Asymmetric Catalysis, vol. II, Springer, Berlin, 1999, p. 650.

[8] (a) M. Yamakawa, H. Ito, R. Noyori, J. Am. Chem. Soc. 122 (2000) 1466;
(b) K. Abdur-Rashid, A.J. Lough, R.H. Morris, Organometallics 19 (2000) 2655;
(c) D.G.I. Petra, J.N.H. Reek, J.-W. Handgraaf, E.J. Meijer, P. Dierkes, P.C.J. Kamer, J. Brussee, H.E. Schoemaker, P.W.N.M. van Leeuwen, Chem. Eur. J. 6 (2000) 2818.

[9] M. Palucki, N.S. Finney, P.J. Pospisil, M.L. Güler, T. Ishida, E.N. Jacobsen, J. Am. Chem. Soc. 120 (1998) 948.

[10] M. Faure, A. Tesouro Vallina, H. Stœckli-Evans, G. Süss-Fink, J. Organomet. Chem. 621 (2001) 103.

[11] G. Süss-Fink, in: W.A. Herrmann (Ed.), Synthetic Methods of Organometallic and Inorganic Chemistry (Catalysis), vol. 10, G. Thieme Verlag, Stuttgart, 2002, p. 123.

[12] (a) G. Süss-Fink, M. Faure, T.R. Ward, Angew. Chem. 114 (2002) 105;
(b) G. Süss-Fink, M. Faure, T.R. Ward, Angew. Chem. Int. Ed. 41 (2002) 99.

[13] G. Laurenczy, M. Faure, L. Vieille-Petit, G. Süss-Fink, T.R. Ward, Adv. Synth. Catal. 344 (2002) 1073.

[14] (a) M.A. Bennett, J.P. Ennett, K.I. Gell, J. Organomet. Chem. 233 (1982) C17;
(b) M.A. Bennett, J.P. Ennett, Inorg. Chim. Acta 198–200 (1992) 583.

[15] M. Jahncke, G. Meister, G. Rheinwald, H. Stœckli-Evans, G. Süss-Fink, Organometallics 16 (1997) 1137.

[16] M. Stebler-Röthlisberger, W. Hummel, P.A. Pittet, H.-B. Bürgi, A. Ludi, A.E. Merbach, Inorg. Chem. 27 (1988) 1358.

[17] S. Tsuzuki, K. Honda, T. Uchimaru, M. Mikami, K. Tanabe, J. Am. Chem. Soc. 124 (2002) 104.

[18] M.A. Bennett, T.-N. Huang, T.W. Matheson, A.K. Smith, Inorg. Synth. 21 (1982) 74.

[19] Y. Miyaki, T. Onishi, H. Kurosawa, Inorg. Chim. Acta 200–302 (2000) 369.

[20] A.J. Birch, J. Chem. Soc. (1950) 1951.

[21] G.M. Sheldrick, Acta Crystallogr. A 46 (1990) 467.

[22] G.M. Sheldrick, SHELXL-97, University of Göttingen, Göttingen, Germany, 1999.

[23] L.J. Farrugia, J. Appl. Cryst. 30 (1997) 565.